



Short communication

## A simple solvent method for the recovery of $\text{Li}_x\text{CoO}_2$ and its applications in alkaline rechargeable batteries



Yanan Xu, Dawei Song, Li Li, Cuihua An, Yijing Wang\*, LiFang Jiao, Huatang Yuan

Institute of New Energy Material Chemistry, Collaborative Innovation Center of Chemical Science and Engineering (Tianjin), Key Laboratory of Advanced Energy Materials Chemistry (MOE), Tianjin Key Lab of Metal and Molecule-based Material Chemistry, Nankai University, Tianjin 300071, PR China

### HIGHLIGHTS

- A simple solvent method using DMF is proposed for recovery of waste  $\text{Li}_x\text{CoO}_2$ .
- This method is simply operated, low-cost and fit for practical application.
- Recovered  $\text{Li}_x\text{CoO}_2$  is studied as anode material of alkaline secondary battery.
- Effect of S-doping on performance of recovered  $\text{Li}_x\text{CoO}_2$  electrode is studied.
- The maximum capacity of  $\text{Li}_x\text{CoO}_2 + 1\% \text{S}$  electrode is 357 mAh g<sup>-1</sup> at 100 mA g<sup>-1</sup>.

### ARTICLE INFO

#### Article history:

Received 26 September 2013

Received in revised form

13 November 2013

Accepted 13 November 2013

Available online 28 November 2013

#### Keywords:

Lithium cobalt oxide

Recovery

Solvent method

Alkaline secondary battery

Anode material

### ABSTRACT

A simple solvent method is proposed for the recovery of waste  $\text{Li}_x\text{CoO}_2$  from lithium-ion batteries, which employs inexpensive DMF to remove the binder of PVDF. This method is convenient to manipulate and low-cost to apply. Electrochemical investigations indicate that recovered  $\text{Li}_x\text{CoO}_2$  materials with a small amount of S-doping exhibit excellent properties as negative materials for alkaline rechargeable Ni/Co batteries. At the discharge current density of 100 mA g<sup>-1</sup>, the  $\text{Li}_x\text{CoO}_2 + 1\% \text{S}$  electrode displays the max discharge capacity of 357 mAh g<sup>-1</sup> and outstanding capacity retention rate of 85.5% after 100 cycles. It could overcome not only the sophisticated, energy-intensive shortcomings of conventional recycling methods, but also the high-cost restriction on alkaline rechargeable Ni/Co batteries.

© 2013 Elsevier B.V. All rights reserved.

## 1. Introduction

The unprecedented energy crisis and environmental deterioration in modern society urgently force us to exploit renewable and green energy sources. Owing to the popularization of portable electronic devices and electric vehicles in actual life, there has been a rapid increase in the demand for Li-ion batteries (LIBs), which exhibit high energy density and efficiency. Therefore, the recycling of waste materials for lithium ion batteries has aroused tremendous attention, on account of environmental contamination and security risks [1–6]. Currently,  $\text{LiCoO}_2$  has been served as the leading cathode material for commercialized LIBs due to excellent electrochemical performance, high energy density and ease

manufacture [7]. The increasing number of depleted  $\text{Li}_x\text{CoO}_2$  materials, however, brings out several adverse points, such as limited cobalt resources, pollution and toxicity. Except for a portion of waste  $\text{Li}_x\text{CoO}_2$  scraps from spent LIBs, the other parts, discarded in the production and performance testing process of LIBs, is also causing ignored damages to the society [8].

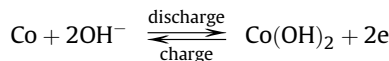
Therefore, it is urgent and significant to take up an in-depth study on the recycling of depleted  $\text{Li}_x\text{CoO}_2$ . As a whole, the existing recycling processes are paying excessive attention on the recovery of noble metal Co and the second synthesis of  $\text{Li}_x\text{CoO}_2$ . Consequently, it causes recovered processes to become sophisticated, energy-intensive, time-consuming and expensive. So the conventional recycling processes are not well considered and far from being well established. An economical, green and facile recovery route for the waste  $\text{Li}_x\text{CoO}_2$  materials should be developed and proposed. Solvent method for the reutilization of  $\text{Li}_x\text{CoO}_2$  through simply removing PVDF is rarely reported. Common

\* Corresponding author.

E-mail address: [wangyj@nankai.edu.cn](mailto:wangyj@nankai.edu.cn) (Y. Wang).

solvents which can dissolve PVDF include N,N-Dimethylformamide (DMF), N-methyl-2-pyrrolidone (NMP) and Dimethylacetamide (DMAc). Then DMF is ultimately chosen in our present work because of low cost, high solubility and reusability.

In addition, a new type Ni/Co battery system has been systematically proposed and received widespread attention [9], which displays higher energy density and better cycle stability than commercial Ni/MH battery and can be denoted as the green battery compared to the toxic features of Ni/Cd battery [10]. Substantial research results from our group have verified the validity of the above conclusions, using Co and Co-X materials (X = OH, S, B, P, O et al.) [11–16] as anode materials for alkaline Ni/Co batteries. The dominant surface faradaic reaction on Co-based electrode can be expressed as follows:



However, high cost of the reported Co-based materials has restricted their application. So we should pay more attention on seeking recovered Co-based materials to reduce the expense of alkaline rechargeable Ni/Co batteries. As we all know, cathode scraps of LIBs necessarily contain abundant resources of  $\text{LiCoO}_2$  materials with small amount of acetylene black and PVDF. Recovered  $\text{Li}_x\text{CoO}_2$ , a kind of layered cobalt oxides, could solve high-cost issue of Co-based materials for Ni/Co batteries by a large margin. Meanwhile, carbon materials have excellent electroconductibility, thus, they are in favor of electrochemical properties for alkaline secondary batteries [11,17]. Therefore, we focus only on the removing of PVDF from  $\text{Li}_x\text{CoO}_2$  scraps of LIBs through a convenient method.

Herein, an economical and convenient solvent method for the recovery and reutilization of  $\text{Li}_x\text{CoO}_2$  is proposed for possible application as anode material of alkaline secondary batteries. The

inexpensive and reusable N,N-Dimethylformamide (DMF) is simply employed to remove PVDF and recover  $\text{Li}_x\text{CoO}_2$  scrap materials.

## 2. Experimental

### 2.1. Materials

Lithium ion batteries (Prismatic Mobile Phone Batteries) discarded in the performance testing process are from Tianjin Lishen Battery Jiont-Stock Co. Ltd. Commercial  $\text{LiCoO}_2$  is acquired from Tianjin B&M Science and Technology Joint-Stock Co. Ltd. N, N-Dimethylformamide (DMF, Tianjin Fengchuan Chemical Reagent Science And Technology Co. Ltd) is employed as recovered solvent.

### 2.2. Experimental procedure

Fig. 1 shows a flowsheet of solvent method designed in this work.  $\text{Li}_x\text{CoO}_2$  cathode scraps binding on Al foil were obtained through manually dismantling and disassembling lithium-ion batteries to remove both plastic gasket and steel cases that cover the batteries. The scraps were immediately placed in organic DMF solvent under fierce stirring at room temperature. When  $\text{Li}_x\text{CoO}_2$  scrap materials were entirely dropped off from Al foil, PVDF was largely dissolved in DMF solvent. And DMF solvent could be recyclable until reaching saturation and it also greatly reduced the budget of recycling process. The obtained scrap sediments were filtered with ethanol and dried in a vacuum at 80 °C. Then they were smashed by a 300 mesh screen to remove residual Al foil fragments. Subsequently,  $\text{LiCoO}_2$  scraps recovered by solvent method were heat-treated at 250 °C, 300 °C and 350 °C for 1 h, respectively, to restore layer structure of  $\text{Li}_x\text{CoO}_2$ . A series of  $\text{Li}_x\text{CoO}_2 + x\% \text{S}$  mixtures ( $x = 1, 2, 5, 10$ ) are prepared by simply

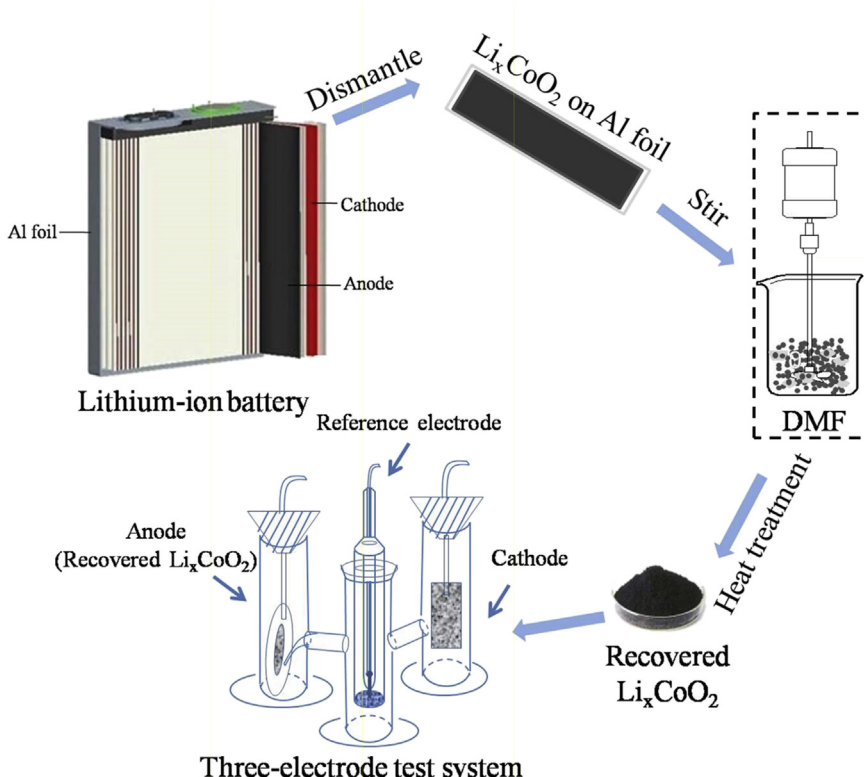


Fig. 1. An entire flowchart of the proposed  $\text{Li}_x\text{CoO}_2$  recovery process. A simple solvent method using DMF to remove PVDF is marked in dashed boxes.

mixing of recovered  $\text{Li}_x\text{CoO}_2$  and S powder under different mass ratios to form uniform powder mixture.

### 2.3. Compositional and structural characterization

The crystal structure and surface morphology of materials were characterized by X-ray diffraction (XRD, Rigaku MiniFlexII with  $\text{Cu K}\alpha$  radiation), Scanning Electron Microscopy (SEM, SUPRA 55VP Field Emission), Thermogravimetric Analysis (TG, NETZSCH TG209), Fourier Transform Infrared Spectroscopy (FTIR-650) and Elemental Analysis (EA, vario EL CUBE).

### 2.4. Electrochemical measurements

Electrochemical measurements were conducted in a three-electrode test system (Fig. 1) using a Land battery test instrument (CT2001A). The  $\text{NiOOH}/\text{Ni}(\text{OH})_2$  electrode and  $\text{Hg}/\text{HgO}$  electrode in a 6 M KOH aqueous solution were served as the cathode electrode and the reference electrode, respectively. Negative electrodes were fabricated with smearing method. They were constructed by mixing as-prepared material with carbonyl nickel powders in a weight ratio of 2:3 to form a paste and coated on a piece of Ni-foam. The electrodes were charged at  $500 \text{ mA g}^{-1}$  for 72 min and discharged to  $-0.5 \text{ V}$  (vs.  $\text{Hg}/\text{HgO}$ ) at the different discharge current density

(100, 200, 500  $\text{mA g}^{-1}$ ) after resting for 5 min. Zahner IM6e electrochemical workstation was used for cyclic voltammetry (scan rate:  $0.2 \text{ mV s}^{-1}$ ; potential interval:  $-1.3 \text{ V}$  to  $-0.4 \text{ V}$  vs.  $\text{Hg}/\text{HgO}$ ). All the tests were performed at room temperature.

## 3. Results and discussion

Considering the crystal form of  $\text{Li}_x\text{CoO}_2$  may be partly destroyed during the recovery processes [5], heat treatment process is designed to improve crystal form. Fig. 2(f) shows TG-DTG curve of PVDF and it starts to decompose at  $400 \text{ }^\circ\text{C}$ . Therefore, in order to avoid and reduce side reaction between  $\text{Li}_x\text{CoO}_2$  and HF produced by the decomposing of PVDF, the temperature of heating treatment should be controlled below  $400 \text{ }^\circ\text{C}$ . Thus,  $250 \text{ }^\circ\text{C}$ ,  $300 \text{ }^\circ\text{C}$  and  $350 \text{ }^\circ\text{C}$  are chosen as heating temperature in this experiment.

### 3.1. Material characterization

The scanning electron microscopy (SEM) images in Fig. 2(a–d) correspond to morphologies of DMF-treated  $\text{Li}_x\text{CoO}_2$  scraps under different-temperature heating treatment (unheated,  $250 \text{ }^\circ\text{C}$ ,  $300 \text{ }^\circ\text{C}$  and  $350 \text{ }^\circ\text{C}$ ), respectively. As the temperature rises, particle size of  $\text{Li}_x\text{CoO}_2$  scraps remains little changed, but particle dispersion significantly increases. It may give rise to the decreasing

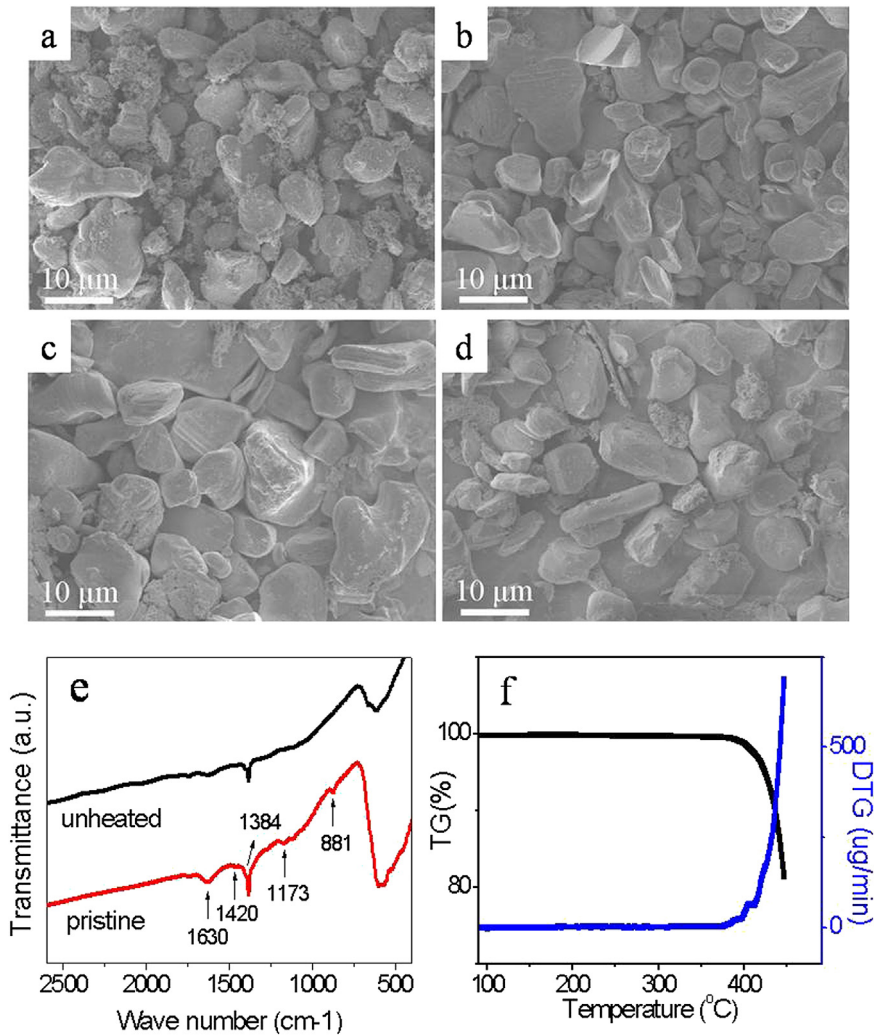


Fig. 2. SEM images of  $\text{Li}_x\text{CoO}_2$  scraps under different temperature treatment (unheated (a)  $250 \text{ }^\circ\text{C}$  (b)  $300 \text{ }^\circ\text{C}$  (c) and  $350 \text{ }^\circ\text{C}$  (d)). (e) IR spectra of unheated scrap materials. (f) TG-DTG curve of PVDF.

of materials conductivity and degenerating of electrochemical performance. The loose part remarked in white rectangle (Fig. 2(a)) is considered as acetylene black. And its content lessens with the increase of temperature, which is consistent with the results of Element Analysis. The carbon content of different-temperature treated  $\text{Li}_x\text{CoO}_2$  scraps (unheat-treated, 250 °C, 300 °C and 350 °C) is 21.91%, 11.94%, 5.86% and 4.11%, respectively. Fig. 2(e) presents IR spectrums of pristine scrap materials directly dismantled from LIBs and unheated scrap materials recovered through solvent method. For the pristine one, there are characteristic absorption peaks of PVDF at 1630  $\text{cm}^{-1}$ , 1420  $\text{cm}^{-1}$ , 1173  $\text{cm}^{-1}$  and 881  $\text{cm}^{-1}$  and the peak intensity of unheated scrap materials is obviously decreased after DMF treatment, indicating that most of PVDF in the scrap materials is removed using solvent method. The absorption peaks of 1384  $\text{cm}^{-1}$  is assigned to the existing of  $\text{NO}_3^-$  from the impurity of KBr.

Fig. 3 shows XRD patterns of  $\text{Li}_x\text{CoO}_2$  scrap materials heated at different temperatures. According to previous literatures [18–21], high ratio of  $I_{003}/I_{104}$  would indicate that the improving of  $\text{Li}_x\text{CoO}_2$  layer structure.  $I_{003}/I_{104}$  values of the pristine and different-temperature heated scrap materials are given in Table 1. The ratio of  $\text{Li}_x\text{CoO}_2$  scrap materials reduces from 3.98 to 1.93 after recovered with DMF. It is further confirmed that crystal form of  $\text{Li}_x\text{CoO}_2$  may be partly destroyed during recovery processes. And the ratio values of recovered  $\text{Li}_x\text{CoO}_2$  after heat treatment are considerably increased, demonstrating that heat treatment contributes to restore the layer structure of  $\text{Li}_x\text{CoO}_2$ . However, when heating temperature rises to 350 °C,  $I_{003}/I_{104}$  ratio decreases to 1.89, which is even lower than that of the unheated one. It illustrates that too high temperature may lead to further damage of  $\text{Li}_x\text{CoO}_2$  scrap materials. We speculate that the main reason may be attributed to side reaction of  $\text{Li}_x\text{CoO}_2$  and HF caused by the decomposition of retained PVDF near 400 °C.

### 3.2. Electrochemical performance

A series of experiments with different conditions have been carried out to determine the optimal temperature and time of heat-treating process and the appropriate additive amount of S powder. Firstly, heating temperature has a significant influence on electrochemical properties of  $\text{Li}_x\text{CoO}_2$  scrap materials under unchangeable heating time. Among them,  $\text{Li}_x\text{CoO}_2$  materials obtained at 300 °C display the maximum discharge capacity of 218  $\text{mAh g}^{-1}$  and preferable capacity retention rate of 73.4% after 100 cycles

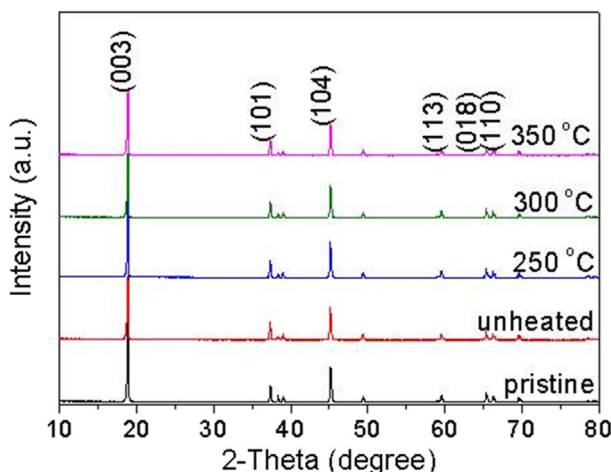


Fig. 3. XRD patterns of  $\text{Li}_x\text{CoO}_2$  scrap materials heating at different temperatures.

**Table 1**  
 $I_{003}/I_{104}$  value of pristine  $\text{Li}_x\text{CoO}_2$  scraps and recovered  $\text{Li}_x\text{CoO}_2$  scraps heating at different temperatures.

$\text{Li}_x\text{CoO}_2$ scraps	$I_{003}/I_{104}$
Pristine	3.98
Unheated	1.93
250 °C	2.21
300 °C	2.02
350 °C	1.89

(Fig. 4(a)). The contributing factor could be that heat treatment is able to restore layer structure of  $\text{Li}_x\text{CoO}_2$  scraps, but exceedingly high temperature may cause active materials serious scatter and secondary damage, leading to performance degradation as aforementioned in Fig. 3. Thus, the optimum temperature is chosen as 300 °C. In addition, time-dependent experiments are also carried out. As shown in Fig. 4(b), electrochemical properties of  $\text{Li}_x\text{CoO}_2$  electrodes gradually become unsatisfactory with the prolonging of heated time. Therefore, the appropriate time of heat-treating process has been confirmed as 1 h.

Electrochemical properties of  $\text{LiCoO}_2$  materials can be greatly enhanced with the doping of S powder [22]. Cycle performances of  $\text{Li}_x\text{CoO}_2 + x\%$  S mixture electrodes at high discharge current density of 500  $\text{mA g}^{-1}$  are shown in Fig. 4(c). Among these electrodes, the  $\text{Li}_x\text{CoO}_2 + 5\%$  S mixture electrode exhibits the maximum discharge capacity of 306  $\text{mAh g}^{-1}$ . Meanwhile, the  $\text{Li}_x\text{CoO}_2 + 1\%$  S mixture electrode shows the most outstanding cycle performance with a capacity retention rate of over 85.3% after 100 cycles. This is because the dissolution of S powder in KOH aqueous solution brings new interspaces among active materials and contact area between active material and alkaline solution [23,24]. Thus, the utilization of active material is enhanced and the excellent cycling performance is obtained. But the discharge capacity does not always enhance with the increasing content of S powder, because overmuch S-doping creates superabundant interspaces among the active materials and lessen electrical conductivity of active material. The rate capabilities and cycling abilities of the  $\text{Li}_x\text{CoO}_2 + 1\%$  S mixture electrode at different discharge current densities are shown in Fig. 4(d). It is observed that all the electrodes allow an electrochemical activation process before their intrinsic capabilities are realized [20]. At discharge current density of 100  $\text{mA g}^{-1}$ , this electrode displays the max discharge capacity of 357  $\text{mAh g}^{-1}$  and the outstanding capacity retention rate of 85.5% after 100 cycles.

### 3.3. Electrochemical reaction mechanism

Fig. 5(a) shows cyclic voltammetry (CV) curves of the commercial  $\text{LiCoO}_2$  and recovered  $\text{Li}_x\text{CoO}_2$  electrode with the doping of 1% S powder at the 10th cycle. The approximate size of peak areas of above two electrodes adequately illustrate that cycle life of recovered  $\text{Li}_x\text{CoO}_2$  scraps can be comparable with the commercial one. As is conveyed by Fig. 5(b), the recycled  $\text{Li}_x\text{CoO}_2$  electrode performs slightly worse than commercial materials at discharge current density of 500  $\text{mA g}^{-1}$ , but the prominent capacity retention rate of reclaimed  $\text{Li}_x\text{CoO}_2$  materials after 100 cycles should be praised immensely. The discharge capacities of commercial  $\text{LiCoO}_2$  and recovered  $\text{Li}_x\text{CoO}_2$  electrode are improved after S-doping. Also curve shape and peak voltage are analogous to those of hexagonal  $\text{LiCoO}_2$  synthesized by hydrothermal method [22]. Therefore, discharge capacity of the  $\text{Li}_x\text{CoO}_2 + 1\%$  S electrode is mainly attributed to electrochemical redox reaction between Co and  $\text{Co}(\text{OH})_2$  [9,10]. Charge-discharge curves of the undoped  $\text{Li}_x\text{CoO}_2$  electrode and  $\text{Li}_x\text{CoO}_2 + 1\%$  S mixture electrode at discharge current density of 500  $\text{mA g}^{-1}$  are also displayed in Fig. 5(c) and (d),

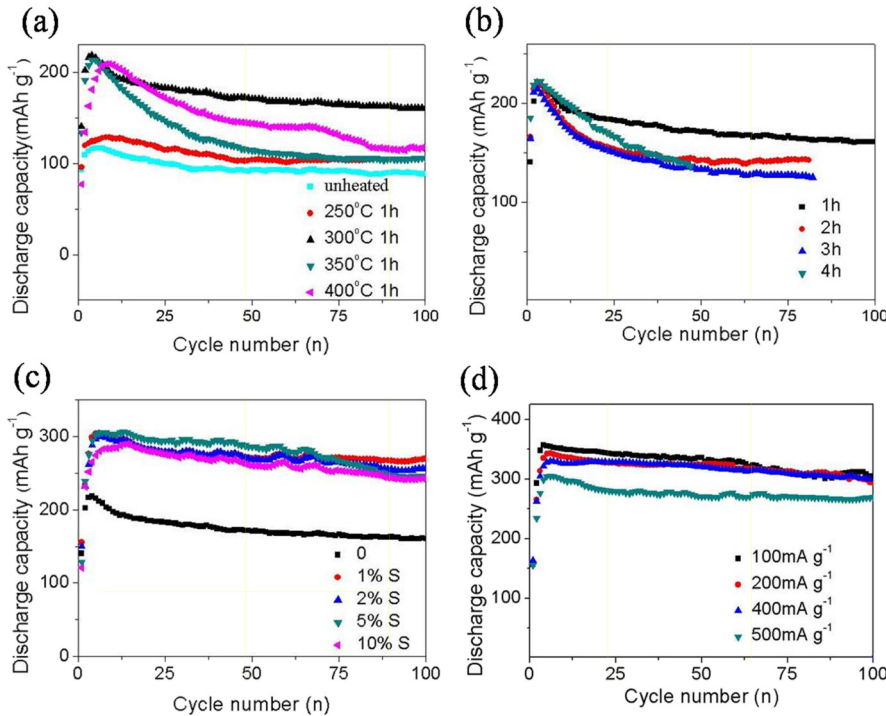


**Fig. 4.** Cycle performances of undoped  $\text{Li}_x\text{CoO}_2$  electrodes heating at different temperatures (a), time (b) and additive content of S powder (c) (discharge current density of  $500 \text{ mA g}^{-1}$ ). Cycle life of  $\text{Li}_x\text{CoO}_2 + 1\%$  S mixture electrode at different discharge current densities (d).

respectively. The discharge potential plateaus of the undoped  $\text{Li}_x\text{CoO}_2$  electrode keeps around  $-0.78 \text{ V}$  (vs.  $\text{Hg}/\text{HgO}$ ) as electrochemical reaction progress, which is also attributed to the transformation from Co to  $\text{Co(OH)}_2$  and accorded with other experimental results [24]. The  $\text{Li}_x\text{CoO}_2 + 1\%$  S electrode presents

the same potential but longer discharging plateau compared with the undoped electrode, which is in good agreement with  $\text{Co(OH)}_2$  mixing with S [12].

Potentiodynamic polarization is employed to investigate the behavior of S powder in the  $\text{Li}_x\text{CoO}_2 + x\%$  S electrode. The

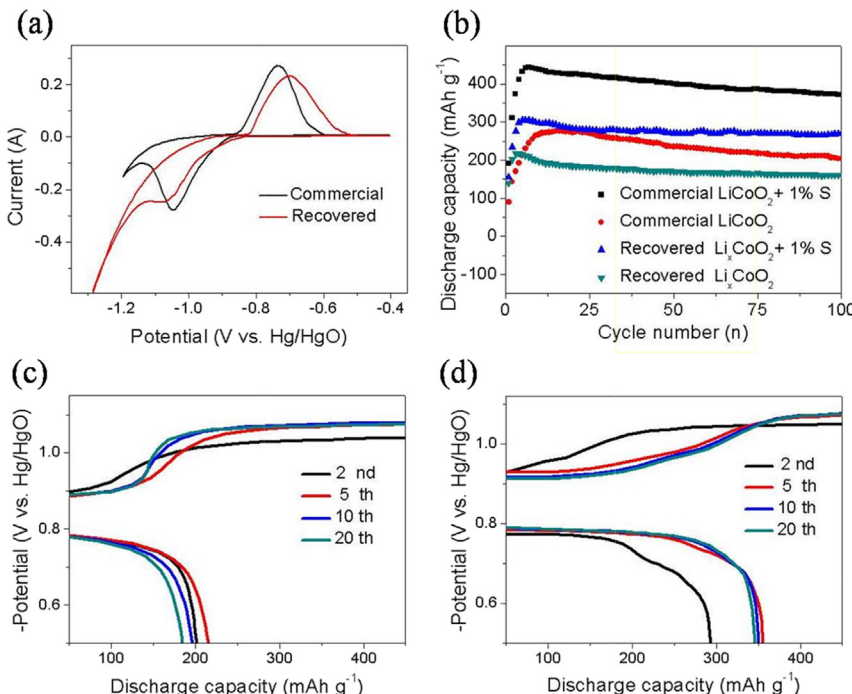


**Fig. 5.** Cyclic voltammetry (CV) curves (a) and cycle performances (b) of the commercial  $\text{LiCoO}_2$  and recovered  $\text{Li}_x\text{CoO}_2$  electrode with the doping of 1% S powder. Charge-discharge curves of the undoped  $\text{Li}_x\text{CoO}_2$  electrode (c) and the  $\text{Li}_x\text{CoO}_2 + 1\%$  S mixture electrode (d) at the different cycles.

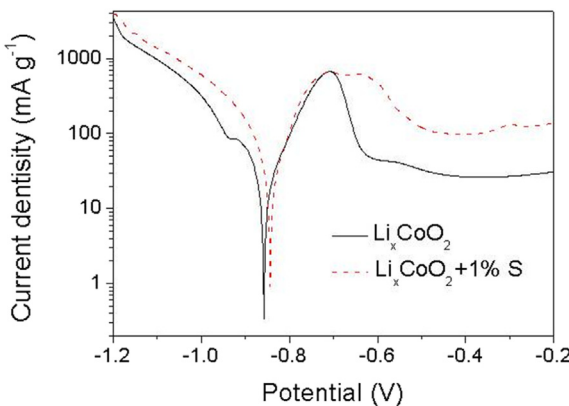


**Fig. 6.** Polarization curves of the undoped  $\text{Li}_x\text{CoO}_2$  electrode and the  $\text{Li}_x\text{CoO}_2 + 1\%$  S electrode.

**Table 2**  
Fitting data of the  $\text{Li}_x\text{CoO}_2$  and  $\text{Li}_x\text{CoO}_2 + \text{S}$  electrodes.

Electrodes	$E_{\text{erro}}$ (V)	$I_{\text{corr}}$ (A)
$\text{Li}_x\text{CoO}_2$	-0.858	0.3412
$\text{Li}_x\text{CoO}_2 + \text{S}$	-0.844	0.9107

polarization curves of undoped  $\text{Li}_x\text{CoO}_2$  electrode and  $\text{LiCoO}_2 + 1\%$  S electrode are shown in Fig. 6. And relevant results obtained by Tafel fitting are summarized in Table 2. After the doping of S powder, the value of the corrosion potential ( $E_{\text{corr}}$ ) slightly decreases and the value of corrosion current ( $I_{\text{corr}}$ ) substantially increases. It suggests that the adding of S improves the corrosion behavior of  $\text{Li}_x\text{CoO}_2$  electrode, that is to say, the dissolution of amorphous S in alkaline solution brings new interspaces among the  $\text{Li}_x\text{CoO}_2 + x\%$  S electrode and increases contact area between electrode material and alkaline electrolyte. This characters result in the improvement of electrochemical properties of the  $\text{Li}_x\text{CoO}_2 + x\%$  S electrode.

#### 4. Conclusions

An economical and facile solvent method for the recovery of high-performance  $\text{Li}_x\text{CoO}_2$  scrap materials may give rise to the potential substitution of conventional recycling routes. Electrochemical investigations indicate that recovered  $\text{Li}_x\text{CoO}_2$  electrodes exhibit favorable properties as negative materials for alkaline rechargeable Ni/Co batteries. At the discharge current density of  $100 \text{ mA g}^{-1}$ , the  $\text{Li}_x\text{CoO}_2 + 1\%$  S electrode displays the max discharge capacity of  $357 \text{ mAh g}^{-1}$  and the outstanding capacity retention rate of 85.5% after 100 cycles. The high discharge capacity,

excellent cycle stability and outstanding rate capability demonstrate that the recovered  $\text{Li}_x\text{CoO}_2$  materials are suitable to be used as negative materials for high power applications. It could overcome not only the sophisticated, energy-intensive shortcomings of conventional recycling method, but the high-cost drawback of alkaline rechargeable Ni/Co batteries.

#### Acknowledgments

This work was financially supported by 973 (2011CB935900, 2010CB631303), NSFC (21231005, 51071087), 111 Project (B12015), Research Fund for the Doctoral Program of Higher Education of China (20120031110001), Nature Science Foundation of Tianjin (11JCYBJC07700) and KLAEMC-OP201101.

#### References

- [1] M.J. Lain, J. Power Sources 97–98 (2001) 736–738.
- [2] J.Y. Chun, M. Chung, J. Lee, Y. Kim, Phys. Chem. Chem. Phys. 15 (2013) 7036–7040.
- [3] C.K. Lee, K.-I. Rhee, J. Power Sources 109 (2002) 17–21.
- [4] J.M. Nan, D.M. Han, M.J. Yang, M. Cui, X.L. Hou, Hydrometallurgy 84 (2006) 75–80.
- [5] J.H. Li, P.X. Shi, Z.F. Wang, Y. Chen, C.-C. Chen, Chemosphere 77 (2009) 1132–1136.
- [6] S.M. Shin, N.H. Kim, J.S. Sohn, D.H. Yang, Y.H. Kim, Hydrometallurgy 79 (2005) 172–181.
- [7] D.-I. Ra, K.-S. Han, J. Power Sources 163 (2006) 284–288.
- [8] L. Li, B.D. Jennifer, X.X. Zhang, L. Gaines, R.J. Chen, F. Wu, K. Amine, J. Power Sources 233 (2013) 180–189.
- [9] X.P. Gao, S.M. Yao, T.Y. Yan, Z. Zhou, Energy Environ. Sci. 2 (2009) 502–505.
- [10] X.Y. Zhao, L.Q. Ma, X.D. Shen, J. Mater. Chem. 22 (2012) 277–285.
- [11] L. Li, Y.N. Xu, C.H. An, Y.J. Wang, L.F. Jiao, H.T. Yuan, J. Power Sources 238 (2013) 117–122.
- [12] D.W. Song, Y.J. Wang, Q.H. Wang, Y.P. Wang, L.F. Jiao, H.T. Yuan, J. Power Sources 195 (2010) 7115–7119.
- [13] Q.H. Wang, L.F. Jiao, H.M. Du, W.X. Pen, D.W. Song, Y.J. Wang, H.T. Yuan, Electrochim. Acta 56 (2011) 1106–1110.
- [14] D.W. Song, Q.H. Wang, Y.P. Wang, Y.J. Wang, Y. Han, L. Li, G. Liu, L.F. Jiao, H.T. Yuan, J. Power Sources 195 (2010) 7462–7465.
- [15] Q.H. Wang, L.F. Jiao, H.M. Du, Q.N. Huan, W.X. Peng, D.W. Song, Y.J. Wang, H.T. Yuan, J. Mater. Chem. 21 (2011) 14159–14162.
- [16] Y. Han, Y.J. Wang, Y.P. Wang, L.F. Jiao, H.T. Yuan, Int. J. Hydrogen Energy 35 (2010) 8177–8181.
- [17] H.M. Du, L.F. Jiao, Q.H. Wang, W.X. Peng, D.W. Song, Y.J. Wang, H.T. Yuan, J. Power Sources 196 (2011) 5751–5755.
- [18] T. Fang, J.-G. Duh, Surf. Coat. Technol. 201 (2006) 1886–1893.
- [19] R.J. Gummow, M.M. Thackeray, I.F. David, S. Hull, Mater. Res. Bull. 27 (1992) 327–337.
- [20] J. Cho, G. Kim, H.S. Lim, J. Electrochem. Soc. 146 (1999) 3571–3576.
- [21] J. Li, E. Murphy, J. Winnick, P.A. Kohl, J. Power Sources 102 (2001) 294–301.
- [22] Y.N. Xu, D.W. Song, J. Li, L. Li, C.H. An, Y.J. Wang, L.F. Jiao, H.T. Yuan, Electrochim. Acta 85 (2012) 352–357.
- [23] D.S. Lu, W.S. Li, X. Jiang, C.L. Tan, R.H. Zeng, J. Alloys Compd. 485 (2009) 621–626.
- [24] Q.H. Wang, L.F. Jiao, H.M. Du, Q.N. Huan, W.X. Peng, D.W. Song, Y.J. Wang, H.T. Yuan, Electrochim. Acta 56 (2011) 4992–4995.